The Ninth Workshop on Digital Fluid Power, September 7-8, 2017, Aalborg, Denmark

ROBUST CONTROL OF DIGITAL HYDRAULIC SERVO ACTUATOR

Matti Linjama
Tampere University of Technology
P.O.BOX 589, FI-33010 Tampere, Finland
E-mail: matti.linjama@tut.fi
Phone: +358 40 8490 525

ABSTRACT

The paper studies robust position and velocity tracking control of a high inertia hydraulic actuator. Fast on/off valves with 3 ms response time are used to implement digital hydraulic valve system. A model-based control approach is used to realize high performance force control, and tracking control is implemented by cascaded velocity and position controllers. Earlier experimental results with cascaded P+PI controller have proven the approach and the focus of this paper is in the improvement of the robustness and performance by using robust control design methods. Simulated results show good tracking performance and excellent robustness against variations in bulk modulus and inertia load. The system remains stable under 407 % increase in the load mass and 50 % reduction in the bulk modulus. The tracking performance with the nominal load mass is comparable to the more advanced control solutions.

KEYWORDS: Digital hydraulics, Robust control, Tracking control

1 INTRODUCTION

Hydraulic servo actuators are used in demanding position, velocity and force control applications [1]. The high-end solutions use symmetric cylinders together with critically lapped symmetric four-way servo valve. Single rod cylinder is more practical solution, but it results in the pressure jump at the zero velocity if controlled by the symmetric servo valve. Cavitation may also occur with overrunning loads. Distributed valves can solve these problems but they often use slow proportional valves and are thus not suitable for demanding control applications [2]. Digital hydraulic valve system is a distributed valve based on on/off valves. Benefits include robustness against oil

impurities and inherent fault tolerance. However, the existing on/off valves are bulky and their response time is relatively long. The best off-the-shelf valves have response time of seven milliseconds with proper power electronics [3, 4], which is far from the response time of the best servo valves. A newcomer is the digital valve system based on miniaturized solenoid valves [5]. The principle is to use mutually similar valves and increase the number of them, which results in smaller valves. Small valve has smaller moving masses and has thus potential for faster response time. The valve package with 64 miniaturized valves was introduced in [6] and the full amplitude response time was three milliseconds only.

Fast distributed digital hydraulic valves allow new type of control solutions for hydraulic actuators. An example of this is given in [7] where a force control solution was developed for high inertia systems. The velocity and position tracking controller was implemented by simple P+PI controller and simulated results showed good performance. Special attention was paid on the robustness of the solution against uncertainty in the load mass, bulk modulus and system delay. The experimental results with another system showed poorer tracking performance [8]. This was probably caused by very big variations in the load mass. This paper studies if it is possible to improve the performance by using rigorous robust control design method instead of robustly tuned P+PI controller.

2 LINEAR MODEL OF THE SYSTEM

2.1 **Controller structure**

The controller structure is shown in Figure 1. The force controller defines the control signals of individual valves such that the force error after one sampling period is minimized, see [8] for details. The force controller needs pressures, piston position and piston velocity as inputs. The velocity and position tracking control is implemented by cascaded velocity and position controllers.

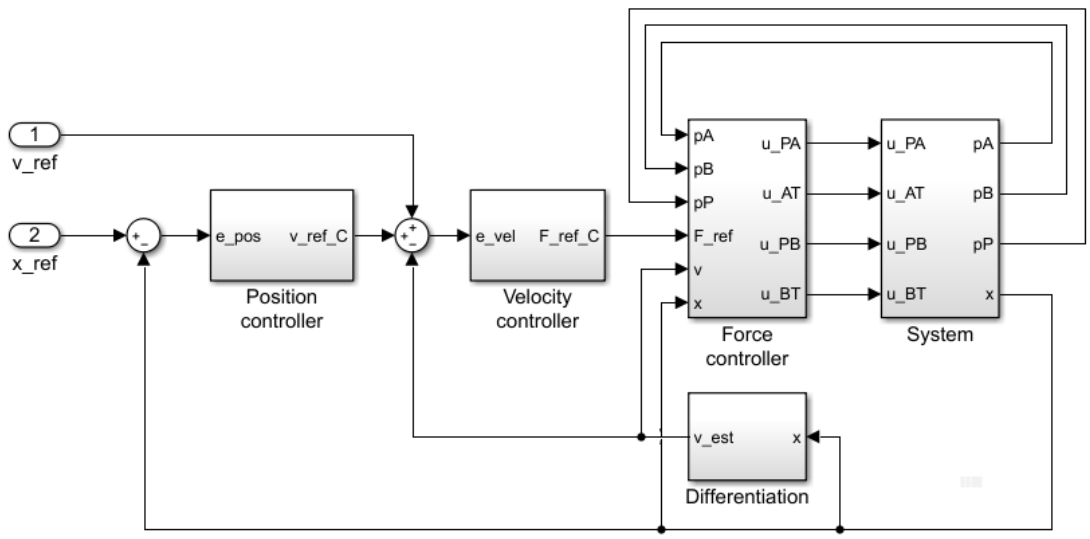

Figure 1. Block diagram of the controller.

2.2 **Continuous time model**

It is shown in [7] that the system dynamics from force reference to piston velocity can be approximated by

$$G_{vel}(s) = \frac{1}{m\,s} G_F(s) e^{-d_T s} \tag{1}$$

where $G_F(s)$ is

$$G_F(s) = \frac{\frac{\tau_B A_A + \tau_A A_B}{A_A + A_B} s + 1}{(\tau_A s + 1)(\tau_B s + 1)} \tag{2}$$

The time constants are given by

$$\tau_A = -\frac{T_S}{\ln\left(1 - B_{eff,A} / \hat{B}_{eff,A}\right)}, \quad \tau_B = -\frac{T_S}{\ln\left(1 - B_{eff,B} / \hat{B}_{eff,B}\right)} \tag{3}$$

where $B_{eff,A}$ and $B_{eff,B}$ are the effective bulk moduli of cylinder chambers and $\hat{B}_{eff,A}$ and $\hat{B}_{eff,B}$ are their estimates. Note that the inner-loop force controller linearizes the system and model is thus linear. This is big benefit when compared to traditional hydraulic servo systems, which are non-linear.

2.3 **Discrete time model**

Robust control design methods yield usually high-order controllers having fast poles. This makes it difficult to discretize them with relatively long sampling period. These problems can be avoided if controller design is made directly in discrete time. The discretization is made by using Tustin's approximation

$$s = \frac{2}{T_S} \frac{z-1}{z+1} \tag{4}$$

The discrete time approximation of the term $1/(m\,s)$ is

$$G_{mz}(z) = \frac{T_S}{2m} \frac{z+1}{z-1} \tag{5}$$

The discretized version of G_F is

$$
\begin{aligned}
num(z) = {} & T_S\left(A_A T_S + 2A_A\tau_B + A_B T_S + 2A_B\tau_A\right)z^2 + \\
& \left(T_S\left(A_A T_S + 2A_A\tau_B + A_B T_S + 2A_B\tau_A\right) + T_S\left(A_A T_S - 2A_A\tau_B + A_B T_S - 2A_B\tau_A\right)\right)z + \\
& T_S\left(A_A T_S - 2A_A\tau_B + A_B T_S - 2A_B\tau_A\right) \\
\\
den(z) = {} & \left(T_S + 2\tau_B\right)\left(T_S + 2\tau_A\right)\left(A_A + A_B\right)z^2 + \\
& \left(\left(T_S - 2\tau_B\right)\left(T_S + 2\tau_A\right) + \left(T_S + 2\tau_B\right)\left(T_S - 2\tau_A\right)\right)\left(A_A + A_B\right)z + \\
& \left(T_S - 2\tau_B\right)\left(T_S - 2\tau_A\right)\left(A_A + A_B\right)
\end{aligned}
\tag{6}
$$

$$
G_{Fz}(z) = \frac{num(z)}{den(z)}
$$

The delay is approximated by the second order Pade approximation

$$
e^{-d_T s} \approx \frac{\frac{d_T^2}{12}s^2 - \frac{d_T}{2}s + 1}{\frac{d_T^2}{12}s^2 + \frac{d_T}{2}s + 1} \tag{7}
$$

The discretized version of the Pade approximation is

$$
G_{dz}(z) = \frac{\left(3T_S^2 - 3T_S d_T + d_T^2\right)z^2 + \left(6T_S^2 - 2d_T^2\right)z + 3T_S^2 + 3T_S d_T + d_T^2}{\left(3T_S^2 + 3T_S d_T + d_T^2\right)z^2 + \left(6T_S^2 - 2d_T^2\right)z + 3T_S^2 - 3T_S d_T + d_T^2} \tag{8}
$$

The complete system model is

$$
G_{vel,z}(z) = G_{mz}(z)G_{Fz}(z)G_{dz}(z) \tag{9}
$$

3 ROBUST CONTROLLER DESIGN

3.1 **Robust control toolbox**

The Matlab version R2016b together with Robust Control Toolbox 6.2 is used. The toolbox offers several functions for robust control design. The functions support both continuous and discrete time design. In this paper, the discrete time mixed sensitivity approach is used.

3.2 **Description of uncertainty**

The parameter uncertainties are the same as in [8]

- m = 10450 – 53000 kg
- d_T = 3 – 8 ms
- τ_A = 0.1 – 8 ms
- τ_B = 0.1 – 8 ms

Note that the parameter variations are exceptionally big. The nominal parameters are selected as follows

$$par_{nom} = k\, par_{min} + (1-k)\, par_{max} \tag{10}$$

where par_{min} and par_{max} are the minimum and maximum values of the parameter *par*, and *k* is a tuning parameter between 0 and 1.

The uncertain parameters are defined in the Robust Control Toolbox by command ureal

```
m = ureal('Mass',m_nom,'Range',[m_min m_max]);
tauA = ureal('tauA',tauA_nom,'Range',[tauA_min tauA_max]);
tauB = ureal('tauB',tauB_nom,'Range',[tauB_min tauB_max]);
d = ureal('Delay',d_nom,'Range',[d_min d_max]);
```

3.3 **Velocity controller**

The P-controller is used in the velocity loop as suggested in [7]. The transfer function from velocity error to force reference is simply gain $K_{P,vel}$. The transfer function from velocity reference to piston position is

$$G_{pos,z}(z) = \frac{G_{vel,z}(z) K_{P,vel}}{1 + G_{vel,z}(z) K_{P,vel}} G_{int}(z) \tag{11}$$

where $G_{int}(z)$ is transfer function of the integrator.

3.4 **Position controller**

3.4.1 Reference controller

The reference controller for the position loop is PI controller [8]

$$G_P(s) = K_{P,pos} + \frac{K_{I,pos}}{s} \tag{12}$$

The controller is discretized by using Tustin's approximation.

3.4.2 Mixed sensitivity design

The mixed sensitivity design is achieved by using command mixsyn. The integrator $G_{int}(z)$ is approximated by a first order model. This is needed in order to avoid failure in the mixsyn function.

$$\frac{1}{s} \approx \frac{1}{s+\varepsilon} \Rightarrow G_{int}(z) = \frac{T_S z + T_S}{(2+\varepsilon T_S) z - 2 + \varepsilon T_S} \tag{13}$$

where ε is small number, 10^{-5} in our case. The position controller $G_{Pz}(z)$ is found by command

```
G_Pz = mixsyn(G_pos_z,W1,W2,W3);
```

where W1, W2 and W3 are the weighting functions, which are used to tune the frequency response of the system. W1 is selected to be large at small frequencies and W3 large at high frequencies. W2 can be ignored or selected as a constant. In our case, the design fails if W2 is omitted and a small constant value of 0.001 is used. The weighting functions are generated by command makeweight

```
W1 = makeweight(1000,omega_1,0.8,T_S);
W3 = makeweight(0.8,omega_3,1000,T_S);
```

where the first input argument is gain at zero frequency, the second input argument is crossover frequency and the third input argument is the gain at high frequencies. The crossover frequencies ω_1 and ω_3 are tuning parameters. The parameter ω_1 must be smaller than ω_3.
The integrator is appended to the controller in order to improve disturbance rejection. This is made by following command

```
G_Pz = G_Pz + K_I*c2d(tf(1,[1 0]),T_S,'tustin');
```

where K_I is the integrator gain.

3.5 **Controller tuning**

3.5.1 Force and velocity controllers

The values of the tuning parameters of the force and velocity controllers are the same as in [8]. The sampling period T_S is 5 ms and the velocity controller gain $K_{P,vel}$ is 450000 Ns/m.

3.5.2 Tuning principles for position controllers

The robust tuning of the position controller is made by analyzing the multiplicative modelling error of the system. The multiplicative modelling error is

$$\Delta_M(z) = \frac{G_T(z) - G_N(z)}{G_N(z)} \tag{14}$$

where G_N is the nominal transfer function and G_T is the true transfer function of the system. The nominal model is obtained from Eq. 11 by using nominal parameter values and the true model is obtained from Eq. 11 by using actual parameter values. The position controlled system remains stable if the nominal closed-loop system is stable, if G_N and G_T have the same number of unstable poles and if following holds [9]

$$\left|\Delta_M(z)\right| < \left|\frac{1 + G_N(z)G_{Pz}(z)}{G_N(z)G_{Pz}(z)}\right| \;\forall\, |z| = 1 \tag{15}$$

The tuning is made by plotting the magnitude of Δ_M with different parameter values and finding position controller such that inequality of Eq. 15 is satisfied. In practice, some margin is needed in Eq. 15 in order to have non-oscillatory response. Also, the margin should increase with frequency in order to have robustness against high frequency modelling errors, such as pipeline dynamics.

Figure 2 presents the multiplicative modelling error for parameters k = 0.8 and T_S = 5 ms. The load mass, time constants and system delay are varied according to Section 3.2. The figure sketches also the "optimal" shape of the right hand side of Eq. 15. The figure shows three targets for the controller design.

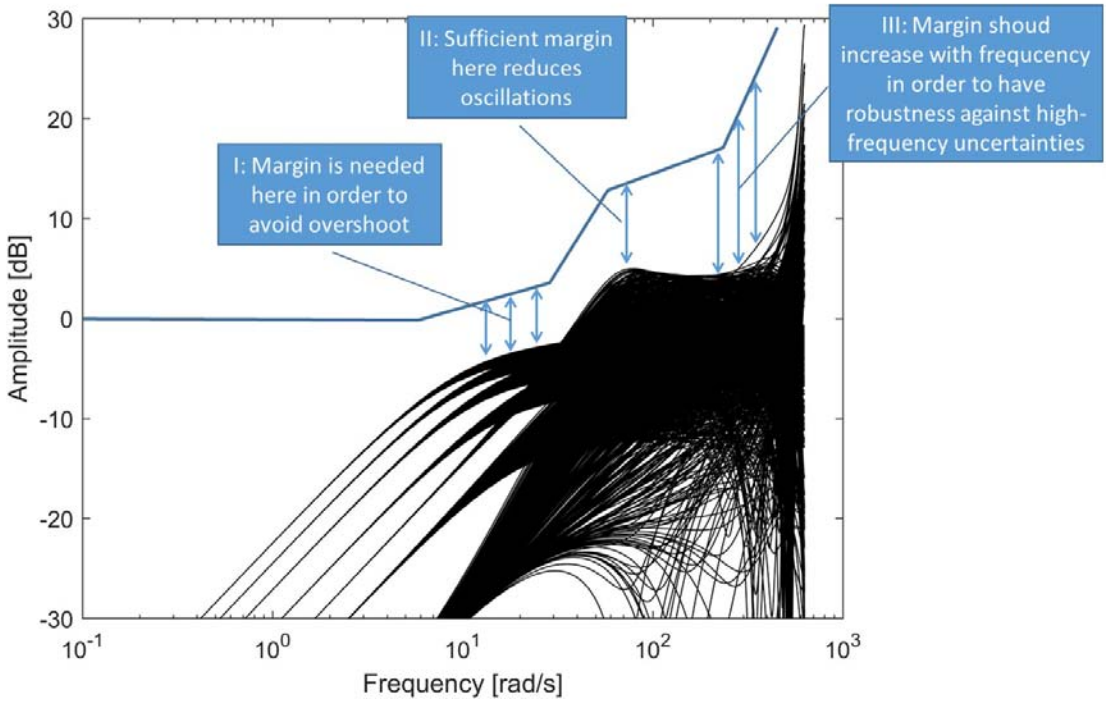

Figure 2. Multiplicative modelling error with parameters k = 0.8 and T_S = 5 ms. The load mass, time constants and system delay have seven equally spaced values with uncertainty range according to Section 3.2.

3.5.3 PI-controller

The PI-controller is tuned according to [8], i.e. K_P = 12 s^{-1} and K_I = 12 s^{-2}. Figure 3 presents the right hand side of Eq. 15 for this controller together with multiplicative modelling error. The figure shows also the closed-loop step responses of the linear model. It is seen that PI controller violates the design Target I of Fig. 2, which results in big overshoot. The controller is also unnecessarily robust against high-frequency uncertainties (Target III). Target II is well satisfied, which means non-oscillatory response.

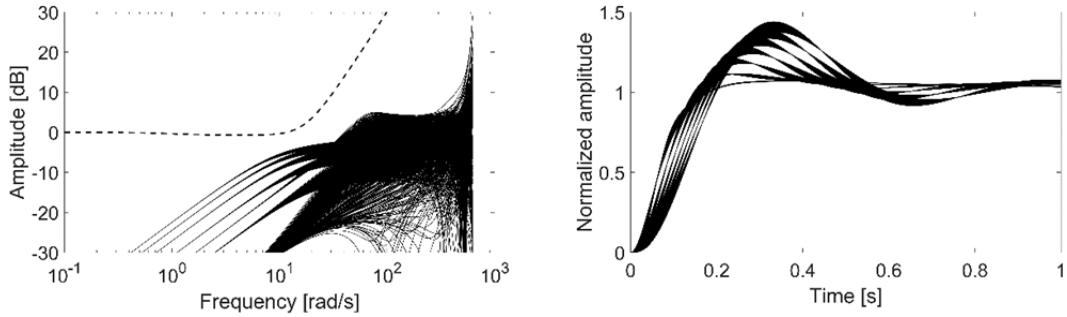

Figure 3. Multiplicative modelling error and RHS of Eq. 15 for the PI controller and corresponding step responses of the closed-loop system. System parameters are varied according to Section 2.3.

3.5.4 Mixed sensitivity controller

The tuning parameters of the mixed sensitivity controller are the crossover frequencies ω_1 and ω_3, and integrator gain K_I. One possible tuning is ω_1 = 15 rad/s, ω_3 = 25 rad/s, K_I = 20 s^{-2}. Figure 4 presents the both sides of Eq. 15 and corresponding step responses. The Target II is slightly violated, which is seen as oscillations at the beginning of the response with certain parameter combinations. Target I is better satisfied than with PI-controller, which results in smaller overshoot.

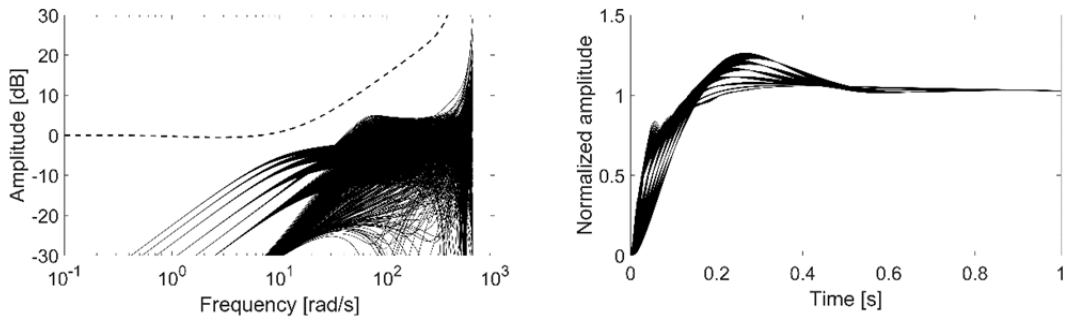

Figure 4. Multiplicative modelling error and RHS of Eq. 15 for the mixed sensitivity controller and corresponding step responses of the closed-loop system. System parameters are varied according to Section 2.3.

4 SIMULATION RESULTS

4.1 Simulation model

The simulation model is a pure inertia system with load mass 10450 or 53000 kg. The model mimics the dynamics of a seesaw mechanism and the dimensions of the mechanism is given in [10]. The load mass 10450 kg is approximately the effective inertia of the mechanism without additional masses and the load mass 53000 kg corresponds the case with additional 200 kg mass at both ends. The dynamics of the load mass is given by

$$
\begin{aligned}
p_A &= \frac{B_A}{A_A x + V_{0A}}\left(Q_{PA} - Q_{AT} - A_A x\right) \\
p_B &= \frac{B_B}{A_B\left(x_{max} - x\right) + V_{0B}}\left(Q_{PB} - Q_{BT} + A_B x\right) \\
mx &= p_A A_A - p_B A_B - F_\mu\left(x\right)
\end{aligned}
\tag{16}
$$

where load force is assumed zero. The cylinder is 63/40-350 and dead volumes V_{0A} and V_{0B} are 0.4 dm^3. Each flow path has 16 parallel connected valves. The flow rates through valves are modelled as follows

$$
Q_{XY} = \sum_{i=1}^{16} \mathbf{u}_{\mathbf{XY}}\left(i\right) K_{v,XY}\,\mathrm{sgn}\left(p_X - p_Y\right)\left(\left|p_X - p_Y\right|\right)^{0.53} \tag{17}
$$

where XY is either PA, AT, PB or BT and i refers to the i:th element of the vector. The valve parameters are $K_{v,PA} = K_{v,PB} = 8.7\times10^{-9}$ $m^3/(s\ Pa^{0.53})$, $K_{v,AT} = K_{v,BT} = 7.5\times10^{-9}$ $m^3/(s\ Pa^{0.53})$. The valve dynamics is modelled as pure delay with 1.5 ms opening delay and 3 ms closing delay. The friction force is given by

$$
F_\mu\left(x\right) = \tanh\left(20000\,\mathrm{m^{-1}s}\cdot x\right)\cdot 1200\,\mathrm{N} + 1000\,\mathrm{Nm^{-1}s}\cdot x \tag{18}
$$

The estimate of the bulk modulus is selected to be 1500 MPa, which is considered as the biggest possible value. The bulk moduli B_A and B_B in the simulation model are assumed either 700 or 1200 MPa. The 700 MPa is considered as the worst case and results in time constants of the pressure dynamics of 8 ms. The value 1200 MPa is more practical and may result in better performance.

4.2 **Simulated responses**

Figure 5 shows the simulated response with 10450 kg load mass and 700 MPa bulk modulus. Controllability is good and there is no hints of instability. Figure 6 presents the response with 10450 kg load mass when bulk modulus is 1200 MPa. The tracking performance is very similar, but pressure dynamics is bit coarser. Figure 7 shows the simulated response when load mass is 53000 kg and bulk modulus is 700 MPa. Tracking error is significantly bigger and small overshoot exists but response is smooth and stable. The response with 1200 MPa bulk modulus is similar and is not presented.

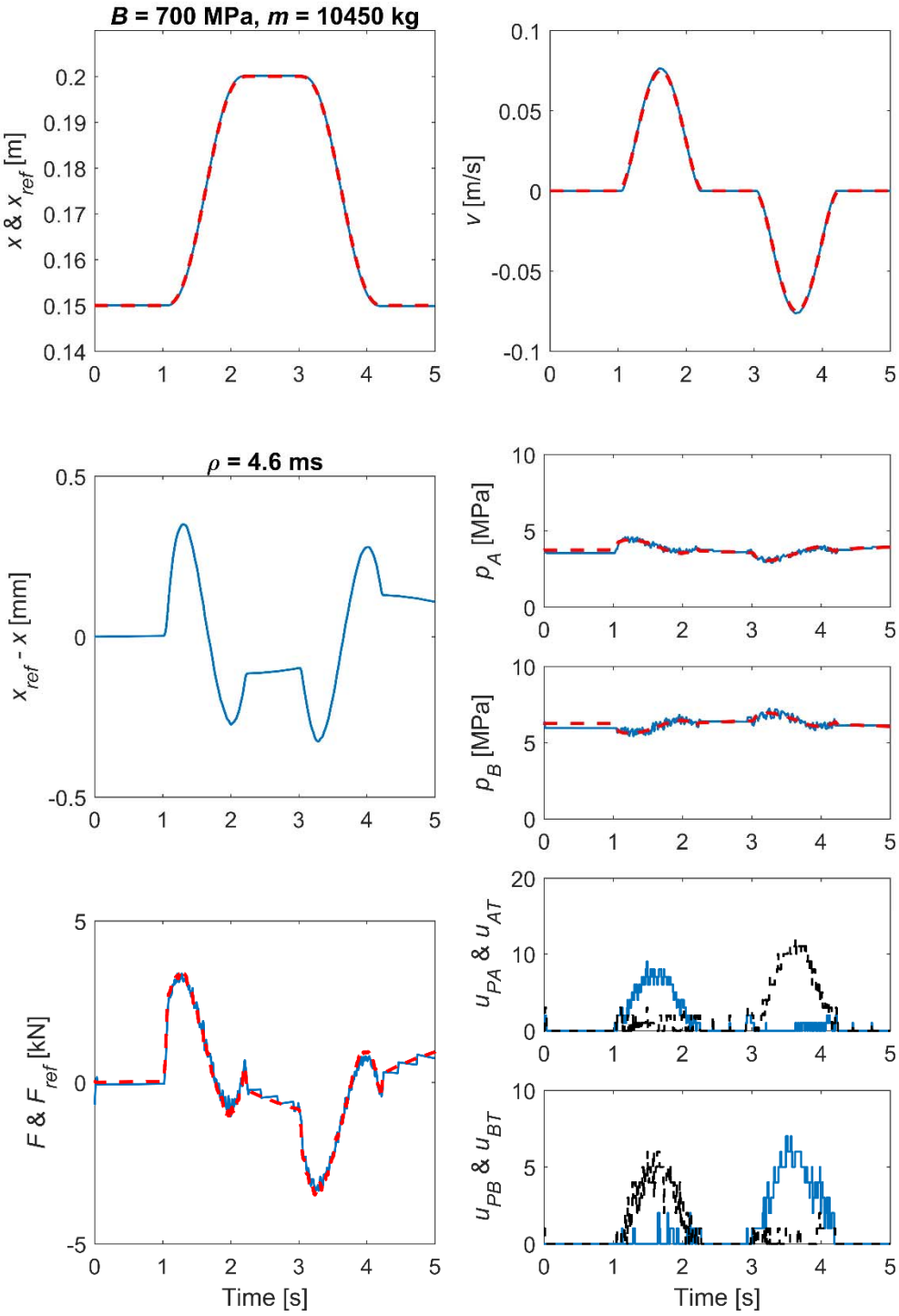

Figure 5. Simulated results with 10450 kg load mass. Bulk modulus is 700 MPa. Target values are shown in red broken line.

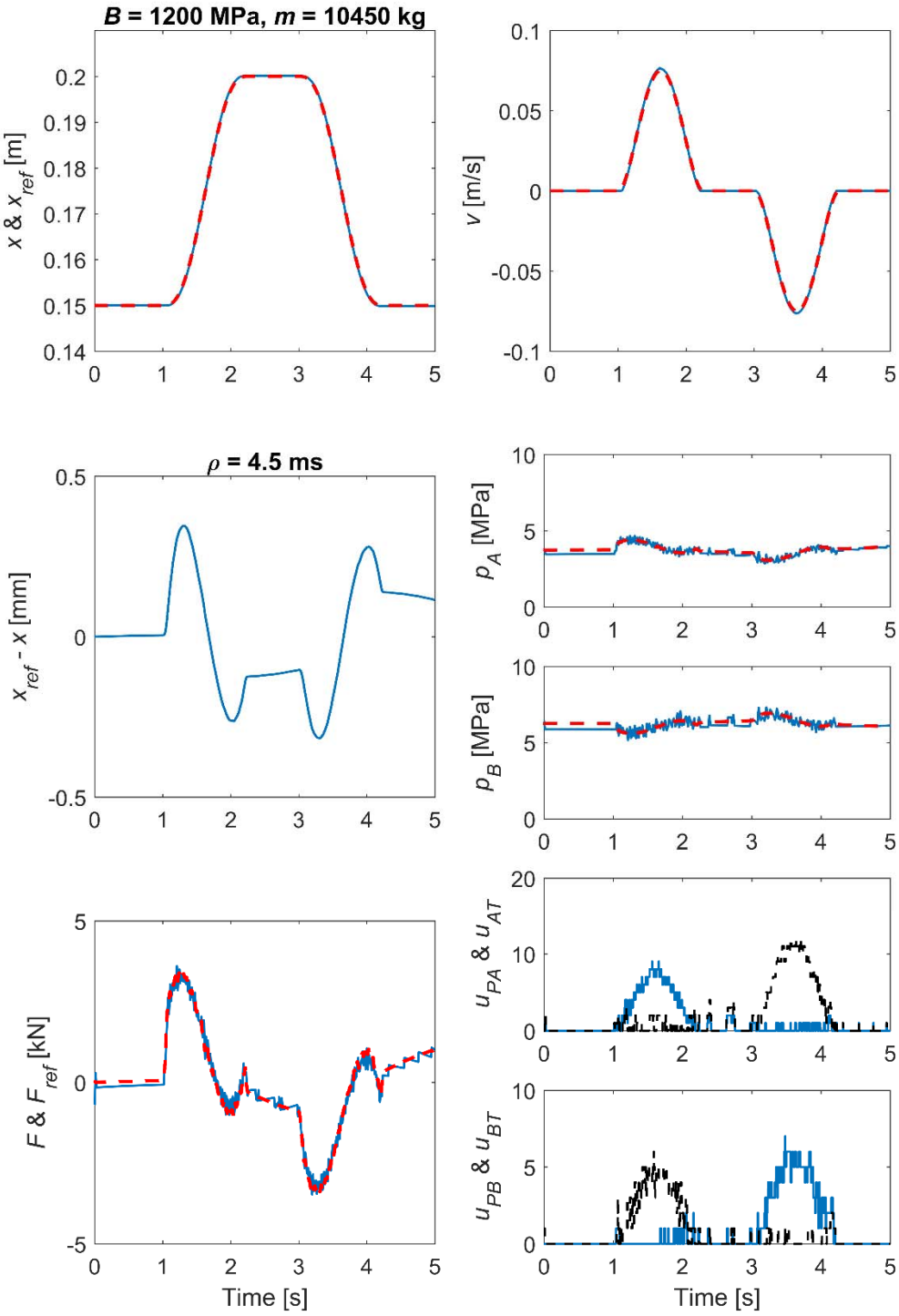

Figure 6. Simulated response with 10450 kg load mass. Bulk modulus is 1200 MPa.

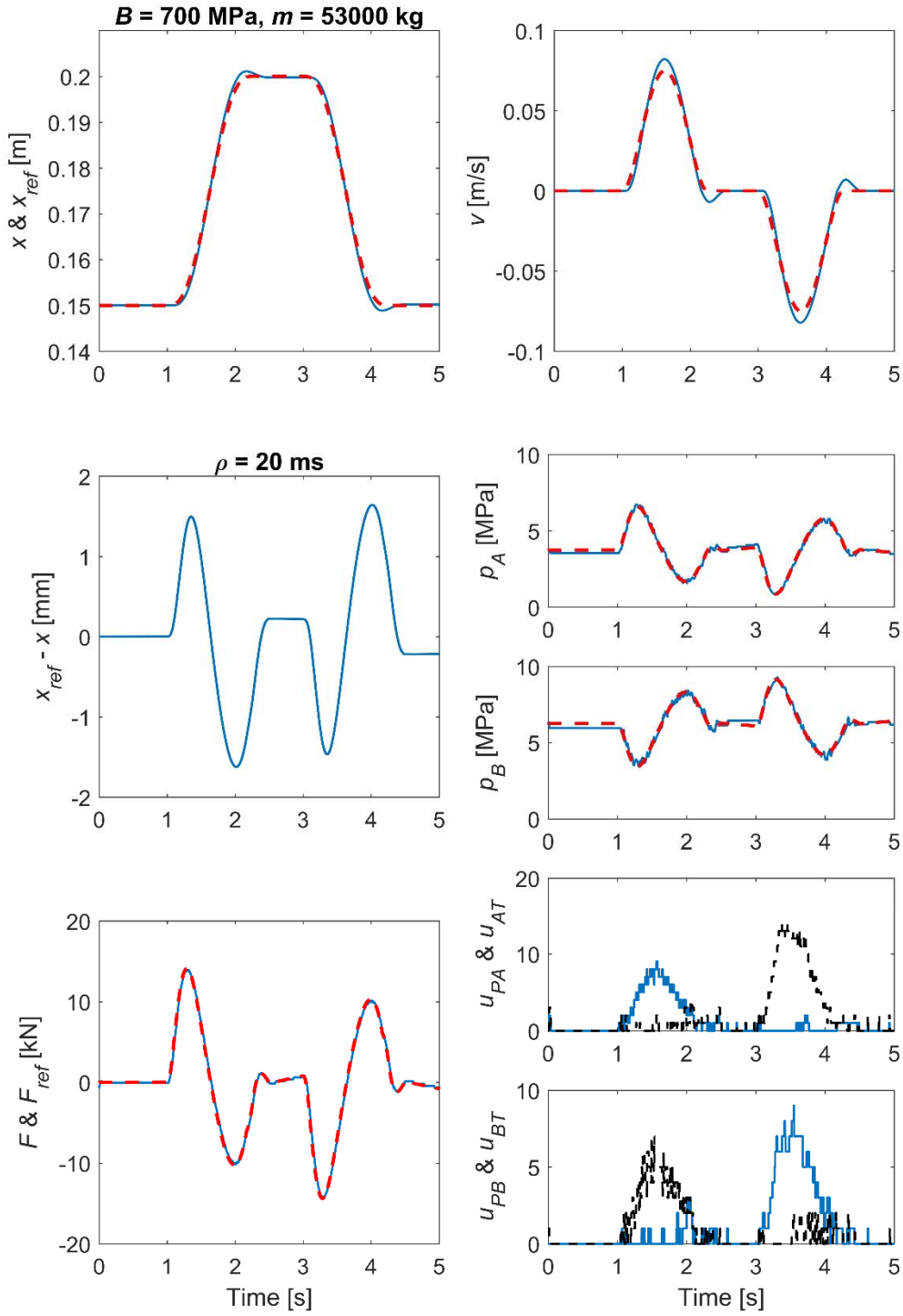

Figure 7. Simulated response with 53000 kg load mass. Bulk modulus is 700 MPa.

5 ANALYSIS OF RESULTS

5.1 **Comparison to PI-controller**

The dynamic performance with PI-controller is quite similar to the mixed sensitivity controller. The biggest differences are in the amount of overshoot and maximum tracking error. Figure 8 compares the tracking error. The mixed sensitivity controller has smaller tracking error.

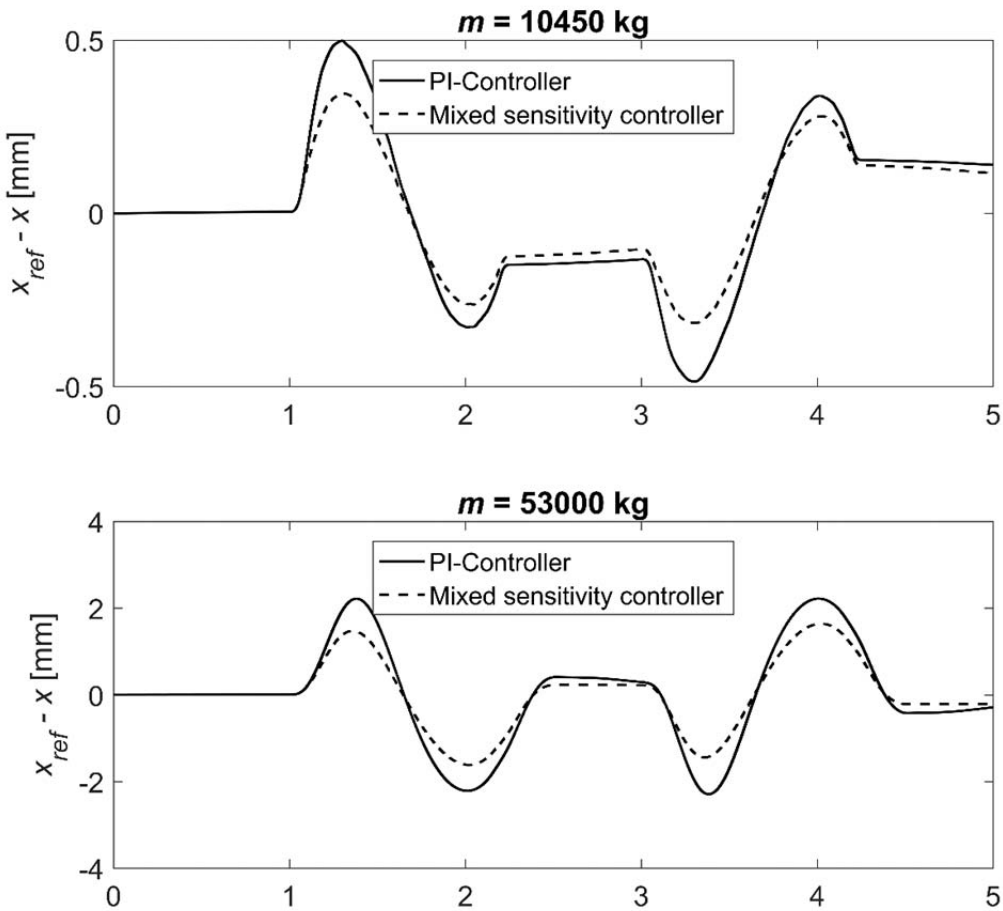

Figure 8. Comparison of tracking errors for PI-controller and mixed sensitivity controller. Bulk modulus is 1200 MPa.

One measure for the tracking performance is the peak position error divided by the peak velocity. This performance index ρ is shown in Table 1 for different cases. The tracking performance is 25-31 percent better with the mixed sensitivity controller. The tracking performance is good with the minimum mass because typical performance index is 3-5 ms with advanced non-linear controllers [11].

Table 1. Tracking performance index for both controllers with different load masses and bulk moduli.

Load mass [kg]	Bulk modulus [MPa]	ρ for Mixed sensitivity controller [ms]	ρ for PI-controller [ms]
10450	700	4.6	6.5
	1200	4.5	6.5
53000	700	20.0	26.7
	1200	19.9	26.4

5.2 **Robustness**

Both controllers are robust against large variations in the bulk modulus and the load mass. The system remains stable even with 407 % increase in the load mass. The large variations in the bulk modulus have practically no effect on performance. This validates the control design approach.

6 CONCLUSIONS

The results reconfirm the fact that the combination of good robustness and performance is possible with the force control approach based on fast digital hydraulic valves. The performance can be improved by using mixed sensitivity approach instead of robustly tuned PI-controller. The tracking error reduces by 25-31 % and overshoot is significantly smaller. On the other hand, PI-controller is easier to tune. Both controllers have very good robustness against variations in the load mass, bulk modulus and system delay.

REFERENCES

1 Jelali, M. and Kroll, A., 2004. Hydraulic servo-systems, modelling, identification and control. London: Springer-Verlag.

2 Eriksson, B. and Palmberg, J.-O. 2011. Individual metering fluid power systems: challenges and opportunities. Proceedings of the Institution of Mechanical Engineers, Part I: Journal of Systems and Control Engineering, Vol. 255, pp. 196–211.

3 Anon. 2010. 3/3, 4/2 and 4/3 directional poppet valve with solenoid actuation, Type SEC. Bosch Rexroth datasheet RE 22035/06.10.

4 Anon. 2015. 2/2 Cartridge Seat Valve, Size 5. Bucher Hydraulics datasheet 400-P-121110-EN-00/09.2015.

5 Paloniitty, M., Linjama. M. & Huhtala, K. 2014. Concept of digital microhydraulic valve system utilising lamination technology. 9th International Fluid Power Conference (9. IFK), Aachen, Germany, 24-26 March 2016, 12 p.

6 Linjama, M., Paloniitty, M., Tiainen, L., Huhtala, K. 2015. Mechatronic Design of Digital Hydraulic Micro Valve Package. Procedia Engineering, Vol. 106, pp. 97–107, doi: 10.1016/j.proeng.2015.06.013.

7 Linjama, M., Huova, M. and Huhtala, K. 2016. Model-based force and position tracking control of an asymmetric cylinder with a digital hydraulic valve. International Journal of Fluid Power, Vol. 17, pp. 163–172.

8 Linjama, M., Huova, M., Karhu, O. & Huhtala. K. 2016. High-Performance Digital Hydraulic Tracking Control of a Mobile Boom Mockup. 10th International Fluid Power Conference (10. IFK), Dresden, Germany, 8-10 March 2016, Paper A-1, 12 p.

9 Åström, K. J. & Wittenmark, B. 1990. Computer-controlled systems, theory and design, second edition. Englewood Cliffs: Prentice-Hall.

10 Huova, M., Aalto, A., Linjama, M., Huhtala, K., Lantela, T. & Pietola, M. 2017. Digital hydraulic multi-pressure actuator – the concept, simulation study and first experimental results. International Journal of Fluid Power, 12 p., doi: 10.1080/14399776.2017.1302775.

11 Mattila J, Koivumäki J, Caldwell D and Semini C. 2017. A Survey on Control of Hydraulic Robotic Manipulators with Projection to Future Trends. IEEE/ASME Transactions on Mechatronics, doi: 10.1109/TMECH.2017.2668604